Check for updates

Received: 9 February 2022 | Revised: 21 June 2022 | Accepted: 6 July 2022

IET Signal Processing

DOI: 10.1049/sil2.12148

The Institution of Engineering and Technology WILEY

ORIGINAL RESEARCH

An improved segmentation technique for multilevel thresholding of crop image using cuckoo search algorithm based on recursive minimum cross entropy

Arun Kumar[1] | Anil Kumar[1] | Amit Vishwakarma[1] | Heung-No Lee[2]

[1]Department of ECE, PDPM Indian Institute of Information Technology Design and Management Jabalpur, Jabalpur, Madhya Pradesh, India

[2]School of Electrical Engineering and Computer Science, Gwangju Institute of Science and Technology, Gwangju, Korea

Correspondence

Anil Kumar, Department of ECE, PDPM Indian Institute of Information Technology Design & Manufacturing Jabalpur, Dumna Airport Road, Jabalpur, Madhya Pradesh, 482005, India.
Email: anilkdee@gmail.com

Abstract

Crop image segmentation is widely used for the analysis of crops. A wide variety of crops are present in the agriculture field, which varies in intensity and complex backgrounds. The thresholding method based on entropy is quite popular for the segmentation of an image. Among all, minimum cross entropy has been widely used. However, the complexity of computation increases when it is used for multilevel thresholding (MLT). Recursive minimum cross entropy is used to resolve the complexity of computation, and cuckoo search (CS) using Levy flight is used to find the optimal threshold for this objective function. Because real-time applications require less processing time while maintaining high performance, which is validated by the CS algorithm using recursive minimum cross entropy (R-MCE-CS) without constraint. The proposed method uses one constraint based on the structural similarity index (SSIM), which leads to an increment in the accuracy for a higher level of thresholding. The accuracy of the proposed method has been tested over 10 crop images with complex backgrounds and high dimensions of colour intensity space. The outcome of the proposed technique has been compared with five algorithms such as wind-driven optimisation (WDO), bacterial foraging optimisation (BFO), differential evolution (DE), artificial bee colony (ABC), and firefly algorithm (FFA). The result shows that the proposed method gives the most promising result, and the accuracy is also improved.

1 | INTRODUCTION

Image Segmentation is a preprocessing step in computer vision technology. The goal of image segmentation is to partition an image into different sections based on its pixel value, colour, and texture to extract meaningful information [1]. A wide variety of crops are present in the agriculture field, which is characterised by irregular spreading in intensity, ambiguity in the background, and weak local pixel correlation which makes it difficult to segment [2–5].

Generally, image processing improves the visual quality of an image. It extracts meaningful data for a variety of applications such as pattern recognition, computer vision, and agricultural applications [6–8]. Mostly, the symptoms of crop disease are visible on the leaf, stem, and fruits. Hence, the disease can be identified by the colour changes on leaves, stems, and fruits [7, 9–11]. The healthy one is identified by changing colour while a drastic change in colour shows an unhealthy one. Primarily, these issues were resolved by agronomists, but with the advent of technology, farmers are able to get predictions about their products in many ways, such as the condition of crop health in advance, ripeness status of fruits or vegetables, and diseases related to crops etc.

In the literature, several approaches for image segmentation have been used [11–15]. Among all, thresholding plays a key role. The thresholding method is divided into two parts: (a) bi-level and (b) multilevel. The bi-level thresholding separates the image into foreground and background in such a way that the separated region would be homogeneous based on texture, edge, and histogram, whereas, an image can be grouped into

This is an open access article under the terms of the Creative Commons Attribution License, which permits use, distribution and reproduction in any medium, provided the original work is properly cited.

© 2022 The Authors. *IET Signal Processing* published by John Wiley & Sons Ltd on behalf of The Institution of Engineering and Technology.

more than two homogenous parts in case of multilevel thresholding (MLT). This is being executed using some criteria, such as minimum entropy, variance minimisation or variance minimisation, etc. for separation of an image. The 2-level thresholding consists of one valley between two peaks, whereas several peaks and valleys are found in MLT [16]. The MLT approach is more complex but the significance is increasing by the day [17, 18]. It also improves the shortcomings of bi-level thresholding methods [3, 16].

Numerous techniques for segmenting colour images have been proposed [3, 19–21]. Otsu *et al.* [22] have proposed a method to partition the greyscale image. Ben *et al.* [23] have proposed a fuzzy C-mean segmentation technique for colour images. Nandhini *et al.* have proposed a method to diagnose the disease on the leaves [24]. However, researchers have received kind attention towards entropy-based thresholding [25–27]. Pare *et al.* [28] have proposed the technique for MLT of colour images using modified fuzzy entropy (MFE). Bhandari *et al.* have proposed the MLT of colour images as well as satellite images using Tsallis entropy and Kapur entropy [29]. Tsalli's entropy [30], Reyni entropy [8], Massi entropy [31], Shannon entropy [32], and cross entropy [33] are types of entropies that can be used to separate the foreground (region of interest) and background of an image. Among all, the minimum cross entropy (MCE) technique is widely used because of its simpler formulation to solve MLT segmentation tasks. It is expressed as a distance in information theory between two probability distributions on the same set. This technique was proposed by Kullback. The optimal value of threshold is found by minimising the cross entropy between the segmented and the original image [33]. The recursive programming reduces the complexity of computation, but as the thresholding level increases, the complexity of computation increases [34]. However, it is a proficient technique for bi-level thresholding. Therefore, a metaheuristic algorithm has been merged with the fitness function (objective function) to increase the computational speed and performance of MLT.

Several optimisation algorithms have been proposed for MLT according to the applications [35, 36]. It is popularly used in image segmentation, but naturally inspired algorithms such as differential evolution (DE) [37], artificial bee colony (ABC) [36], bacterial foraging optimisation [38], wind-driven optimisation (WDO) [39], particle swarm optimisation (PSO) [40], firefly algorithm [41] and cuckoo search (CS) algorithm [42] provide a better result in terms of accuracy and speed of convergence. Yang and Deb [42] developed the CS algorithm, a recent nature-inspired metaheuristic algorithm. Furthermore, instead of simple isotropic random walks, this algorithm utilises the Levy approach, which has better global and local search capability. Mantegna and McCulloch's algorithm is also used by researchers to generate the Levy flight [43, 44]. In addition, the number of tuned parameters in the CS algorithm is very less. As a result, it may be more appropriate for a broader range of optimisation methods. Recent research shows that the CS algorithm outperforms PSO and other genetic algorithms [42]. Recently, Chaturvedi *et al.* [45] have proposed multilevel segmentation of different kinds of fruit images using a modified firefly algorithm.

In this paper, we refer to the technique for MLT of crop images as cuckoo search (CS) via Lévy flight and recursive minimum cross entropy. This technique efficiently searches the optimum threshold value and reduces the complexity of computation. The proposed method uses one constraint based on the SSIM, which leads to an increment in the accuracy for a higher thresholding level. The proposed method has been compared to pre-existing algorithms such as BFO, ABC, WDO, DE, and FFA. The result shows an improvement in accuracy for a higher thresholding level. The rest of the paper is structured as follows: Section 2 introduces the preliminaries along with the mathematical formulation. The review of the CS algorithm is discussed in Section 3. The proposed method has been described in Section 4. Simulation results and comparisons with other segmentation algorithms have been provided in Section 5. Finally, the paper is concluded in Section 6.

2 | PRELIMINARIES

2.1 | Thresholding technique

Thresholding is the basic step for the segmentation of an image. It sets all the pixels above a certain threshold to one and below to zero. Thresholding is categorised into two parts: bi-level and multilevel. In bi-level thresholding, the image can be divided into two parts [34]. Whereas, MLT divides an image into more than two classes (foreground and background). Suppose a greyscale image I of size $M \times N$ is represented with a grey level L (0–255). The MLT finds more than two grey levels to differentiate foreground from the background. The process is executed three times for colour images where each R, G, B channel is taken separately. Numerous techniques have been implemented to find the threshold value globally [18, 30, 46, 47]. The output image is developed according to the multiple threshold values using Equation (1):

$$\begin{aligned} C_0 &= \{I(x,y) \in X | 0 \le I(x,y) \le th_1 - 1\} \\ C_1 &= \{I(x,y) \in X | th_1 \le I(x,y) \le th_2 - 1\} \\ C_i &= \{I(x,y) \in X | th_i \le I(x,y) \le th_{i+1} - 1\} \\ C_k &= \{I(x,y) \in X | th_k \le I(x,y) \le L - 1\}, \end{aligned} \tag{1}$$

In Equation (1), $C_0, C_1, \ldots, C_k$ represents the class separated by a pixel having a threshold value $th_1, th_2, \ldots, th_k$. $I(x,y)$ denotes the pixel intensity of an image related to coordinates x and y . X is the processed image and k is the number of thresholds for which the image has to be partitioned.

2.2 | Structural similarity index

The structural similarity index is used to measure the structural similitude and the structure is compared with the original test image [48].

17519683, 2022, 6, Downloaded from https://ietresearch.onlinelibrary.wiley.com/doi/10.1049/sil2.12148 by Gwangju Institute of Science and Technology (GIST), Wiley Online Library on [05/09/2024]. See the Terms and Conditions (https://onlinelibrary.wiley.com/terms-and-conditions) on Wiley Online Library for rules of use; OA articles are governed by the applicable Creative Commons License

$$SSIM(I_{\text{orgnl}}, I_{\text{Segmt}}) = \frac{\left(2\mu_{I_{\text{orgnl}}}\mu_{I_{\text{Segmt}}} + C_1\right)\left(2\sigma_{I_{\text{orgnl}},I_{\text{Segmt}}} + C_2\right)}{\left(\mu^2_{I_{\text{orgnl}}} + \mu^2_{I_{\text{Segmt}}} + C_1\right)\left(\sigma^2_I + \sigma^2_{I_{\text{Segmt}}} + C_2\right)} \quad (2)$$

In Equation (2), $\mu_{I_{\text{orgnl}}}$ and $\mu_{I_{\text{segmt}}}$ show the mean of the original and segmented image. $\sigma_{I_{\text{orgnl}}}$ and $\sigma_{I_{\text{segmt}}}$ represent the standard deviation of the original image and segmented (outcome) image. $\sigma_{I_{\text{orgnl}},I_{\text{segmt}}}$ is the covariance of the original image and segmented image. The term C_1, C_2 , is set to be 0.6 in our experiment. SSIM is defined for *RGB* images as

$$SSIM = \sum_c SSIM\left(I^c_{\text{orgnl}}, I^c_{\text{segmt}}\right) \quad (3)$$

In Equation (3), $c = 1$ is used for greyscale images, while $c = 1, 2\ and\ 3$ are used for *RGB* images.

2.3 | Multilevel minimum cross entropy

Among various methods of thresholding [1, 3, 16, 22, 49, 50], MCE has been quite popular and is used to select the optimal threshold. It reduces the cross entropy between the segmented and the original test image.

2.4 | Cross entropy

The term cross entropy refers to the relationship between two probability distribution functions $A = \{a_1, a_2, \ldots, a_N\}$ and $B = \{b_1, b_2, \ldots, b_N\}$ and is expressed as

$$D(A,B) = \sum_{i=1}^{N} A^c_i \log \frac{A^c_i}{B^c_i}; c = \begin{cases} 1,2,3 for RGB image \\ 1 for Gray image \end{cases} \quad (4)$$

$$I_{th} = \begin{cases} \mu^c(1,th) I(x,y) < th \\ \mu^c(th, L+1) I(x,y) > th \end{cases} \quad (5)$$

In Equation (5), the original image, histogram, and threshold value computed by integrating three colour components of the cropped image to retain the colour information are represented by $I(x,y)$, $h^c(i)$, and th, respectively, and $\mu^c(r,s) = \sum_{i=r}^{s-1} i h^c(i) / \sum_{i=r}^{s-1} h^c(i)$ respectively. The cross entropy is calculated as

$$D(th) = \sum_{i=1}^{th-1} i h^c(i) \log\left(\frac{i}{\mu^c(1,t)}\right) + \sum_{i=th}^{L} i h^c(i) \log\left(\frac{i}{\mu^c(th, L+1)}\right) \quad (6)$$

After minimising the cross entropy in Equation (6), the optimal threshold is evaluated as

$$t^* = \text{argmin}_t D(t) \quad (7)$$

The computational complexity for n level thresholding is $O(nL^{n+1})$. The computational cost increases when it is prolonged for MLT.

3 | CUCKOO SEARCH ALGORITHM AND LÉVY FLIGHT

Yang and Deb [42] developed the CS algorithm, a recent nature-inspired metaheuristic algorithm The cuckoo is a fascinating bird, not only because it creates decent sound but also because of its aggressive nature of reproduction [51]. The CS is based on some cuckoo species' brood parasitism. Some cuckoo species, namely the ani and guira, put their eggs in communal nests, but they may discard the eggs of others to increase the hatching probability of eggs produced. Generally, CS is used to resolve the structural optimisation issue. There are three basic types of brood parasitism: cooperative breeding, intraspecific brood parasitism, and nest takeover, which simply describe the standard CS. The intruding cuckoos may cause direct conflict with some host birds. Every cuckoo lays one egg at a time and throws it out into the nest in a random way. Some eggs look like the host bird's egg (high-quality egg or solution), which will be handed over to the next generation. The number of host birds is limited. The detected egg is killed, or the host bird discards the nest with a probability P_a that lies between zero and one. The CS algorithm employs a well-balanced combination of local and global explorative random walks, which is governed by p_a(control parameter) [42]. Equation (8) simply describes the local random walk:

Pseudo-code of Cuckoo Search (CS) Algorithm

begin
Objective function $f(x)$, $x=(x_1, \ldots, x_d)^T$;
Initial a population of n host nests x_i $(i=1,2,\ldots,n)$;
while ($fmin$ > tol) or (t<MaxIteration);
Get a cuckoo (k) randomly and generate a new solution by Lévy flights;
Evaluate its quality/fitness; F_k
Choose a nest among n (say j) randomly;
if ($F_k > F_j$),
Replace j by the new solution;
end
Abandon a fraction (P_a) of worse nests
[and build new ones at new locations via Lévy flights];
Keep the best solutions (or nests with quality solutions);
Rank the solutions and find the current best;
end while
end

FIGURE 1 Pseudo-codes of the cuckoo search (CS) algorithm

17519683, 2022, 6, Downloaded from https://ietresearch.onlinelibrary.wiley.com/doi/10.1049/sil2.12148 by Gwangju Institute of Science and Technology (GIST), Wiley Online Library on [05/09/2024]. See the Terms and Conditions (https://onlinelibrary.wiley.com/terms-and-conditions) on Wiley Online Library for rules of use; OA articles are governed by the applicable Creative Commons License

$$x_i(t+1) = x_i(t) + \alpha s \oplus H(p_a - \varepsilon) \oplus (x_j(t) - x_k(t)) \quad (8)$$

In Equation (8), $x_j(t)$ and $x_k(t)$ are two distinct solutions chosen at random by permutation, $H(u)$ represents a Heaviside function, s denotes the step size, and ε is a random number taken from the uniform distribution. Using Levy flights, the global random walk is achieved [34].

$$x_i(t+1) = x_i(t) + \alpha \oplus Lévy(\lambda) \quad (9)$$

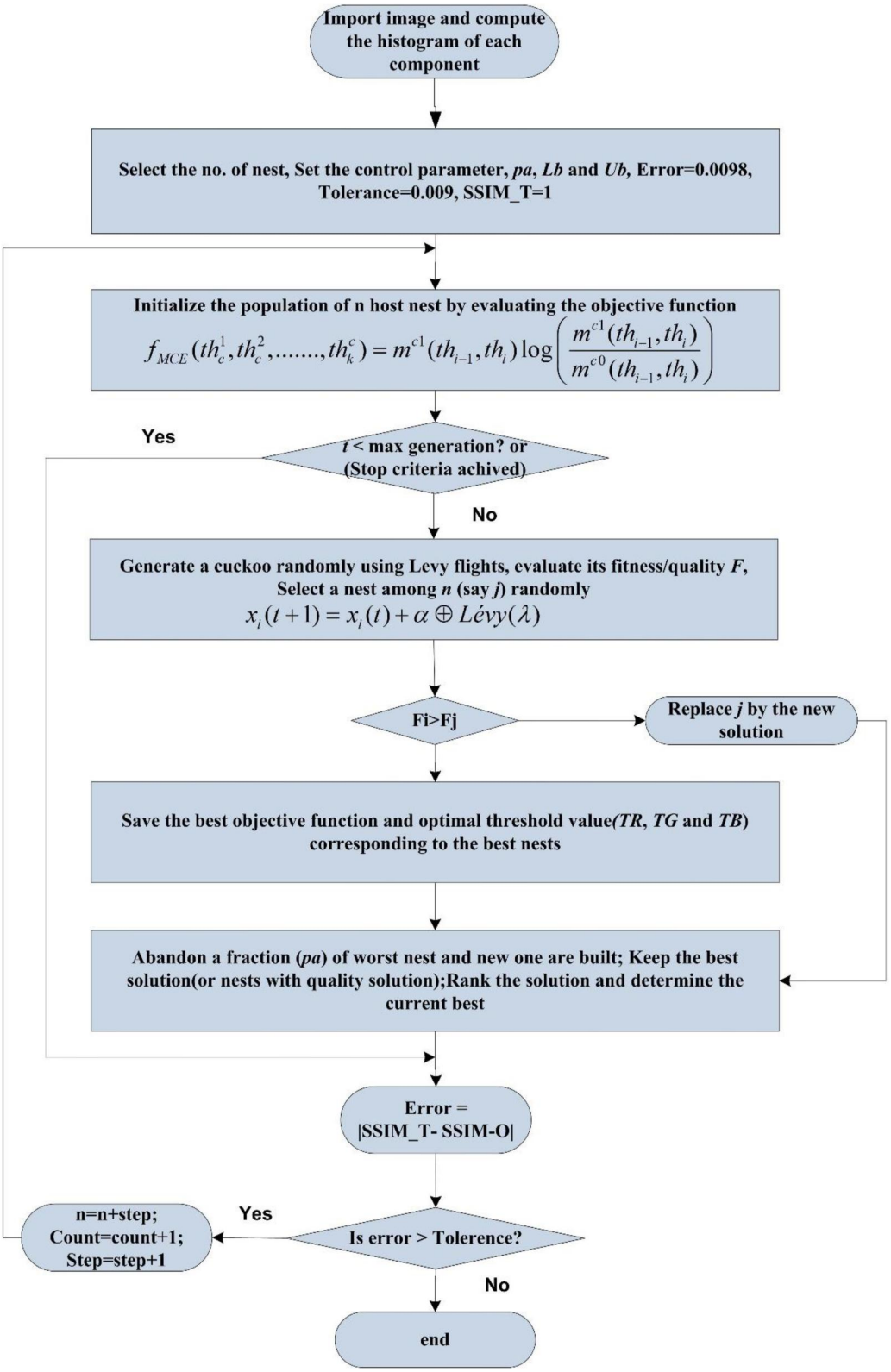

FIGURE 2 Flowchart of the proposed method

17519683, 2022, 6, Downloaded from https://ietresearch.onlinelibrary.wiley.com/doi/10.1049/ipr2.12148 by Gwangju Institute of Science and Technology (GIST), Wiley Online Library on [05/09/2024]. See the Terms and Conditions (https://onlinelibrary.wiley.com/terms-and-conditions) on Wiley Online Library for rules of use; OA articles are governed by the applicable Creative Commons License

In Equation (9), $\alpha(\alpha > 1)$ denotes the step size, $\alpha = 1$ is taken in our case and $\oplus$ is the entry-wise multiplication process. Equation (9) shows the stochastic illustration of a random walk. A stochastic process is a Markov chain in which the next position is determined solely by the current location and the transition probability. Moreover, far-field

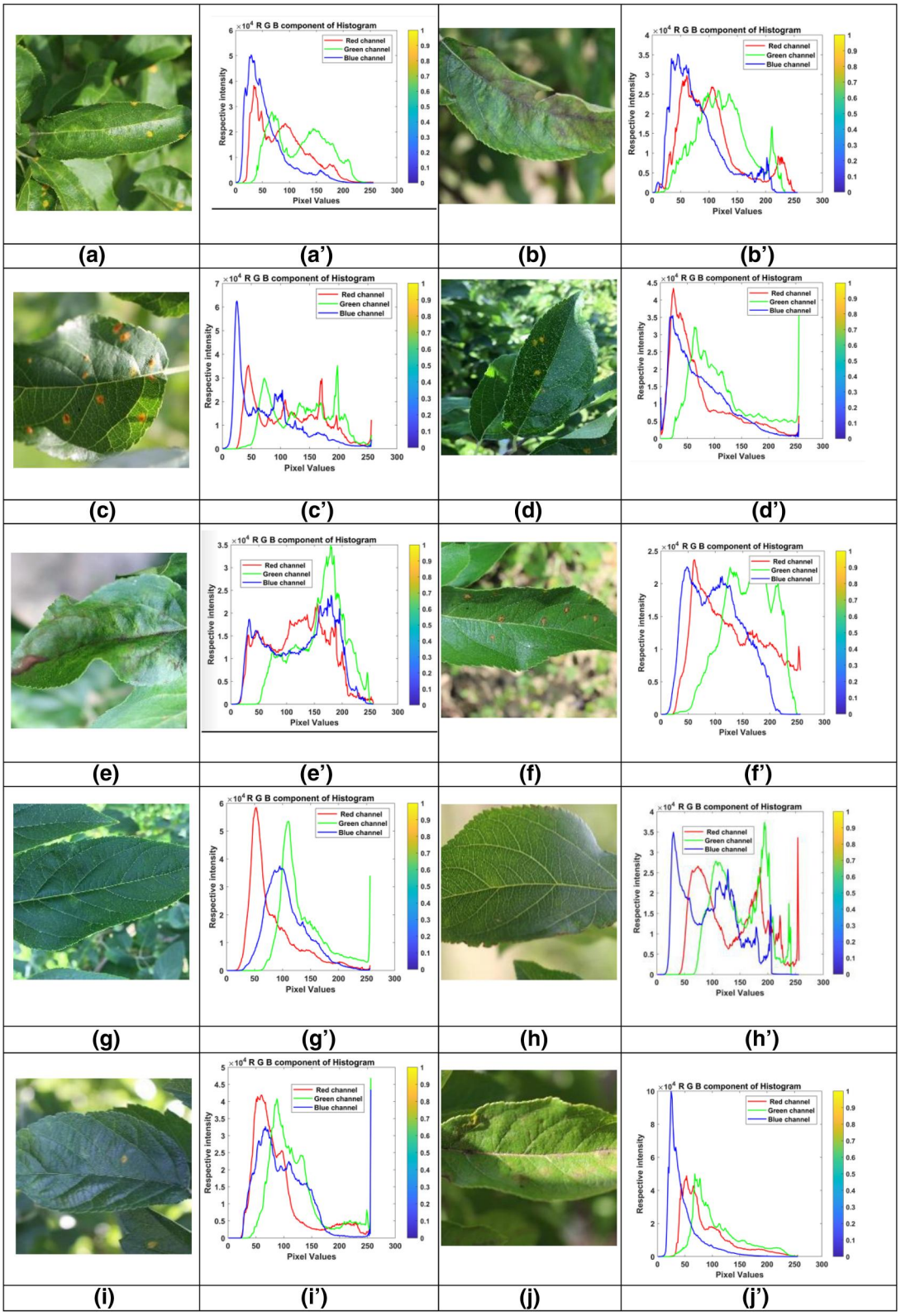

FIGURE 3 Original crop images and their histogram of each colour component

17519683, 2022, 6, Downloaded from https://ietresearch.onlinelibrary.wiley.com/doi/10.1049/sil2.12148 by Gwangju Institute of Science and Technology (GIST), Wiley Online Library on [05/09/2024]. See the Terms and Conditions (https://onlinelibrary.wiley.com/terms-and-conditions) on Wiley Online Library for rules of use; OA articles are governed by the applicable Creative Commons License

randomisation should generate a significant portion of the new solutions, and their locations should be sufficiently distant from the current best solution to ensure that the system does not become stuck in a local optimum. [51, 52]. It is a proficient technique to explore more search areas, which have infinite mean and variance. The Lévy distribution is given as follows:

$$Lévy(\lambda) \sim t^{-\lambda}; 1 < \lambda \leq 3 \tag{10}$$

A variety of nature-inspired metaheuristic algorithms have been used for multilevel thresholding. However, the benefits [26, 42, 51] of using the CS algorithm are as follows:

(a) It is a population-based algorithm. Although the entry-wise product is alike to particle swarm optimisation, a random walk via Lévy flight is more proficient in exploring the search space due to its longer step length in the long and tedious execution.

(b) The parameter is much lower than in PSO, GA, and ABC. As a result, it would be more appropriate for a broader range of optimisation algorithms.

The pseudo-code of the CS algorithm has been presented in Figure 1.

4 | PROPOSED METHOD

In the agriculture world, a wide variety of crops are present in the vicinity and they are varying in intensity with complex backgrounds [2–5]. Hence, MLT is required for the effective and more accurate segmentation of crop images. The minimum cross entropy (MCE) approach is a notable technique for MLT of an image, and the complexity of computation is $O(nL^{n+1})$. Therefore, to reduce the complexity of formulation and increase the accuracy of the segmented image, R-MCE is utilised.

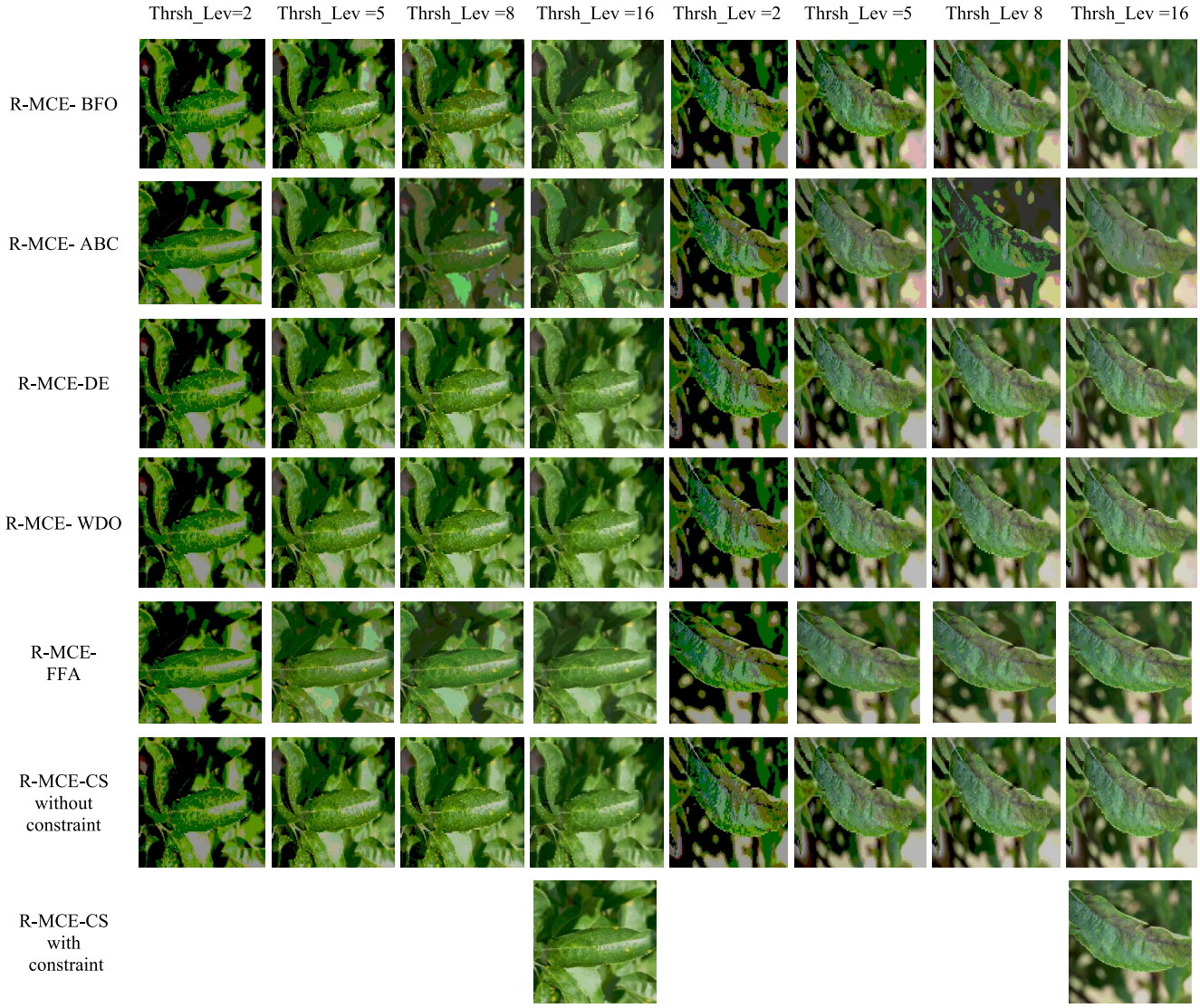

FIGURE 4 Segmented image of crop images (a) and (b) for level 16 based on the proposed technique and other algorithms for levels 2, 5, 8, and 16

17519683, 2022, 6, Downloaded from https://ietresearch.onlinelibrary.wiley.com/doi/10.1049/sil2.12148 by Gwangju Institute of Science and Technology (GIST), Wiley Online Library on [05/09/2024]. See the Terms and Conditions (https://onlinelibrary.wiley.com/terms-and-conditions) on Wiley Online Library for rules of use; OA articles are governed by the applicable Creative Commons License

4.1 | Recursive minimum cross entropy

Recursive minimum cross entropy (R-MCE) is a modified version of MCE. The computational effort of computing gets reduced using recursive programming and it becomes $O(nL^n)$ [49]. It is a straightforward and more accurate method to find the threshold value but it is still a challenging task for MLT. This approach increases the accuracy of the segmented image by minimising the cross entropy between the original and segmented image. The simplified MCE [34, 49] is written in Equation (6) as

$$D(th) = -\sum_{i=1}^{L} ih^c(i)\log(i) - \sum_{i=1}^{th-1} ih^c(i)\log \mu(1, th) - \sum_{i=th}^{L} ih^c(i)\log \mu(th, L+1)) \tag{11}$$

In Equation (11), the first term is constant, so the R-MCE is rewritten as

$$\begin{aligned}\eta(th) &= -\sum_{i=1}^{th-1} ih^c(i)\log \mu(1, th) - \sum_{i=th}^{L} ih^c(i)\log(\mu(th, L+1)) \\ &= -\left(\sum_{i=1}^{th-1} ih^c(i)\right)\log\left(\frac{\sum_{i=1}^{th-1} ih^c(i)}{\sum_{i=1}^{th-1} h^c(i)}\right) - \left(\sum_{i=th}^{L} ih^c(i)\right)\log\left(\frac{\sum_{i=th}^{L} ih^c(i)}{\sum_{i=th}^{L} h^c(i)}\right)\end{aligned} \tag{12}$$

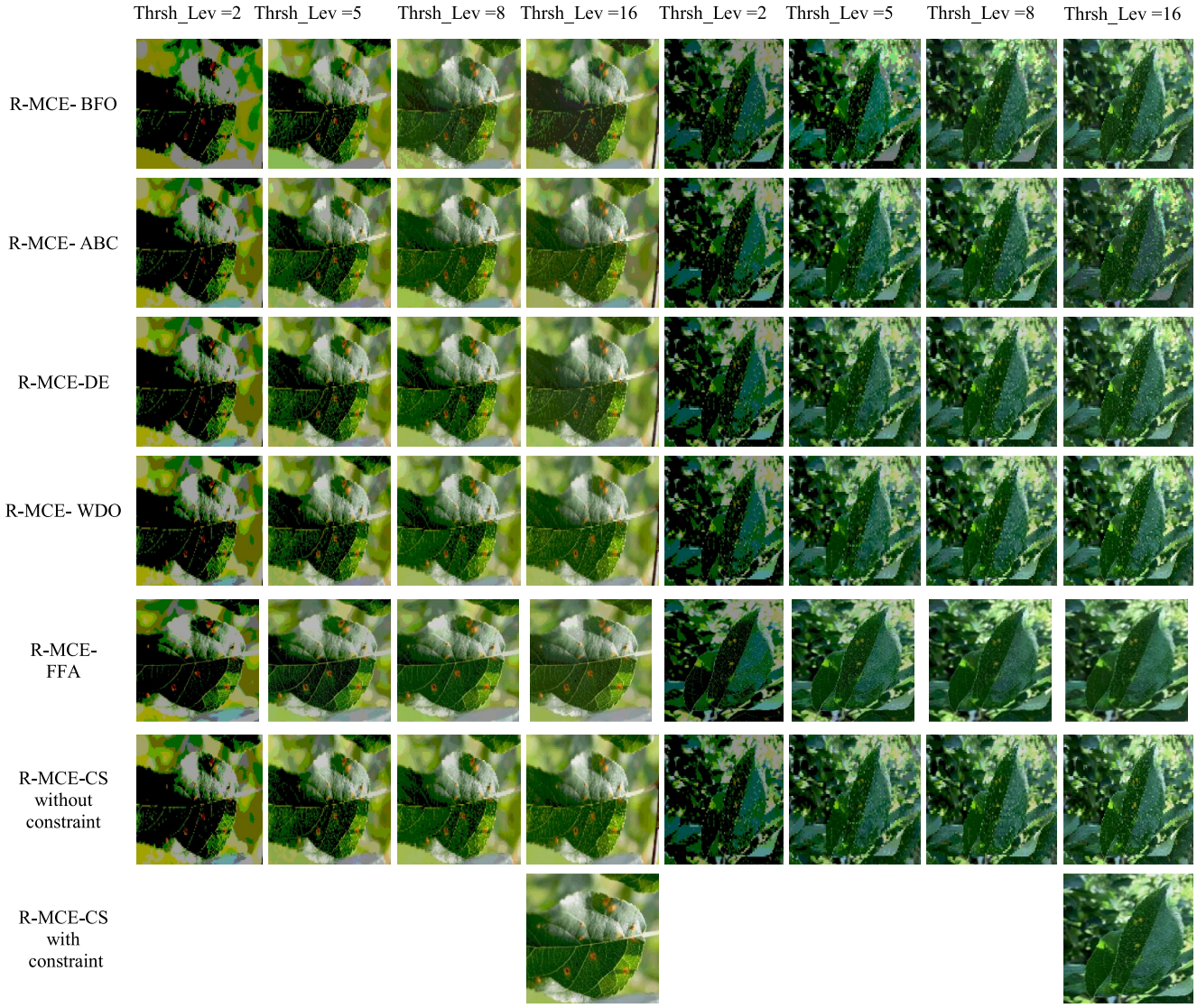

FIGURE 5 Segmented image of crop images (c) and (d) for level 16 based on the proposed technique and other algorithms for levels 2, 5, 8, and 16

17519683, 2022, 6, Downloaded from https://ietresearch.onlinelibrary.wiley.com/doi/10.1049/ipr2.12148 by Gwangju Institute of Science and Technology (GIST), Wiley Online Library on [05/09/2024]. See the Terms and Conditions (https://onlinelibrary.wiley.com/terms-and-conditions) on Wiley Online Library for rules of use; OA articles are governed by the applicable Creative Commons License

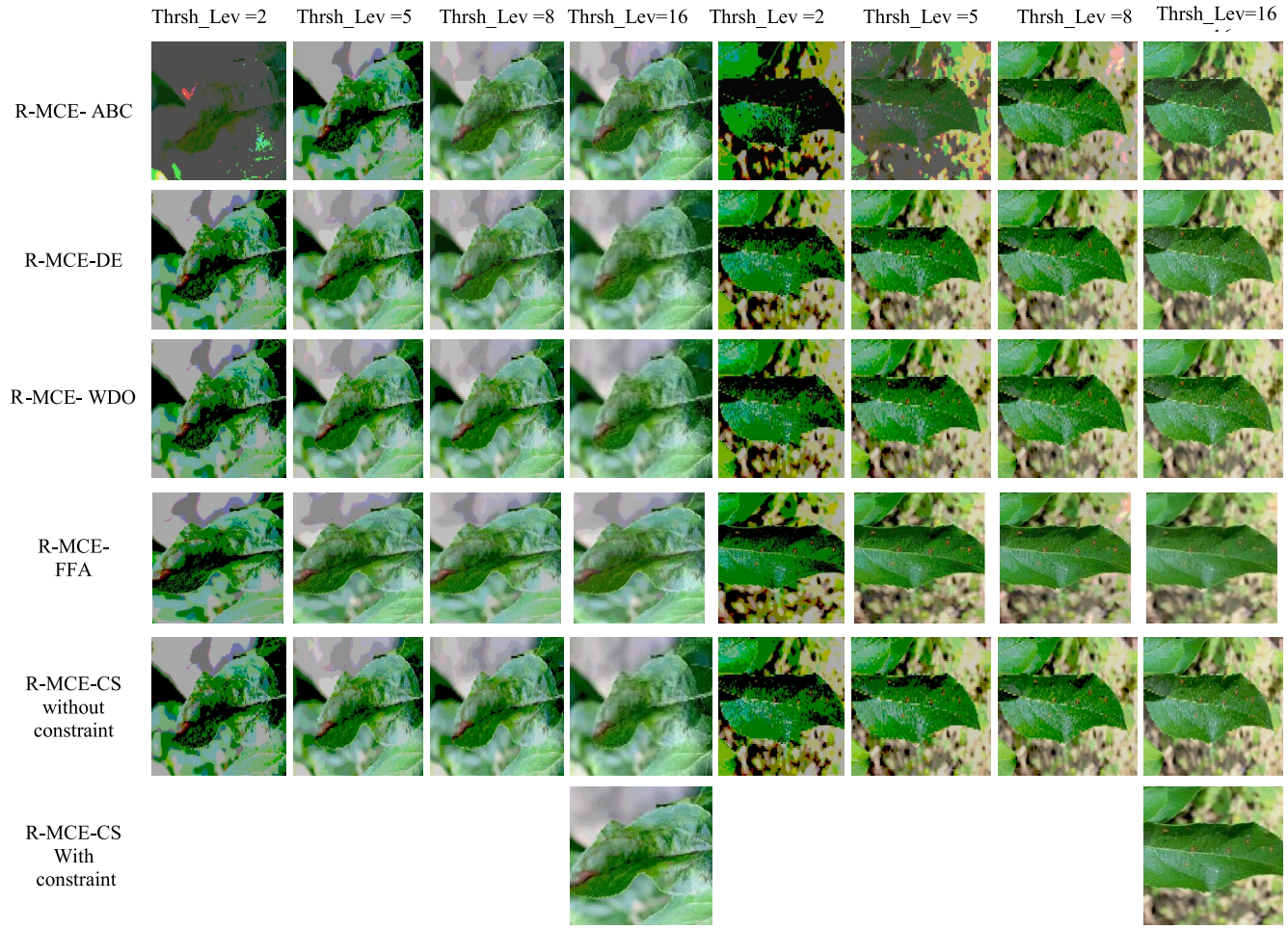

FIGURE 6 Segmented image of crop images (e) and (f) for level 16 based on the proposed technique and other algorithms for levels 2, 5, 8, and 16

$$= -m^{c1}(1, th)\log\left(\frac{m^{c1}(1, th)}{m^{c0}(1, th)}\right) - m^{c1}(th, L+1)\log\left(\frac{m^{c1}(th, L+1)}{m^{c0}(th, L+1)}\right) \quad (13)$$

In Equation (13), m^{c0} and m^{c1} signify the zero and first moment for the histogram of an image. Suppose a crop image I containing L grey-level, N pixel, and k thresholds $th_1, th_2, \ldots, th_k$ is observed for partitioning the original crop image into $k+1$ classes. $th_0 = 0$ and $th_{k+1} = L$ have been carefully chosen, and $th_1 < th_2 <, \ldots, th_k < th_{k+1}$ to epitomise it in the best way. The objective function is expressed in Equation (13) as

$$f_{\mathrm{MCE}}\left(th_c^1, th_c^2, \ldots\ldots, th_k^c\right) = m^{c1}\left(th_{i-1}, th_i\right)\log\left(\frac{m^{c1}(th_{i-1}, th_i)}{m^{c0}(th_{i-1}, th_i)}\right) \quad (14)$$

After minimising Equation (14), the best threshold value can be obtained as

$$\left[t_1^*, t_2^*, \ldots, t_{k-1}^*\right] = \mathrm{argmin}\left\{f_{MCE}\left(th_1^c, th_2^c, \ldots, th_k^c\right)\right\} \quad (15)$$

It is professed that $t_1^* < t_2^* < t_{k-1}^* < L-1$. The greyscale image has a single channel, whereas the colour image has three channels (red, green and blue). The method conferred in Equation (14) is executed three times separately to segment colour crop images. As a result, the segmented image formed by this method is more accurate, but still, it is beneficial for bi-level thresholding. When a mathematical formulation is extended for MLT, each threshold level adds constraint, multimodality, and complexity. Therefore, the objective function is combined with the CS algorithm with Lévy flight to increase the accuracy. This technique can improve the accuracy of segmented images for lower levels as well as the higher level of thresholding. But we aim to improve the accuracy of the segmented image so that it will help the farmer or agriculture industry.

In this paper, recursive minimum cross entropy (R-MCE) and CS algorithm have been combined to choose the optimal threshold value. It minimises the cross entropy between the object of interest and background. The R-MCE-CS technique has been compared with five other metaheuristic algorithms such as WDO, BFO, DE, ABC, and FFA to confirm the accuracy. Secondly, one constraint has been applied in the algorithm section on the SSIM presented in the flowchart of the proposed methodology as shown in Figure 2 for

17519683, 2022, 6, Downloaded from https://ietresearch.onlinelibrary.wiley.com/doi/10.1049/sil2.12148 by Gwangju Institute of Science and Technology (GIST), Wiley Online Library on [05/09/2024]. See the Terms and Conditions (https://onlinelibrary.wiley.com/terms-and-conditions) on Wiley Online Library for rules of use; OA articles are governed by the applicable Creative Commons License

improvement in accuracy. The structural similarity index is a unit of measurement for calculating the similarity between the original and the outcome image. Once the MLT is accomplished on the original images, by using the proposed method with constraint, SSIM provides an idea about the fidelity of the segmented images.

A higher SSIM value indicates better segmentation. This technique is based on error minimisation. The error tends towards zero, or the value of SSIM equal to unity shows a better segmentation. The simulation has been performed on 10 different complex background crop images with a high dimension of colour intensity space. This technique improves fidelity parameters such as mean square error (MSE), peak signal-to-noise ratio (PSNR), feature similarity index (FSIM), and structural similarity index (SSIM). This approach provides a better-segmented image, which leads to an improvement in the accuracy for a higher thresholding level. It added extra benefits in terms of fidelity parameters.

The novelty of this paper is as follows: (a) CS algorithm via Lévy flight has been applied to implement the R-MCE based MLT for crop images, (b) to confirm the accuracy of the proposed method, it was compared to five metaheuristic algorithms: WDO, BFO, DE, ABC, and FFA, and (c) one constraint has been applied on the SSIM, which leads to an improvement in the accuracy for a higher level of thresholding.

5 | EXPERIMENTAL RESULTS

The result and simulation of the proposed method were implemented on Window 10, Intel(R) Core (TM) i7-3770 CPU with a processor speed of 3.40 GHz and 4 GB RAM. MATLAB 2014a has been used to implement the algorithms.

The original crop images and their R, G, and B histogram are shown in Figure 3 which show different histogram characteristics and irregular distribution (abruptly altering the value

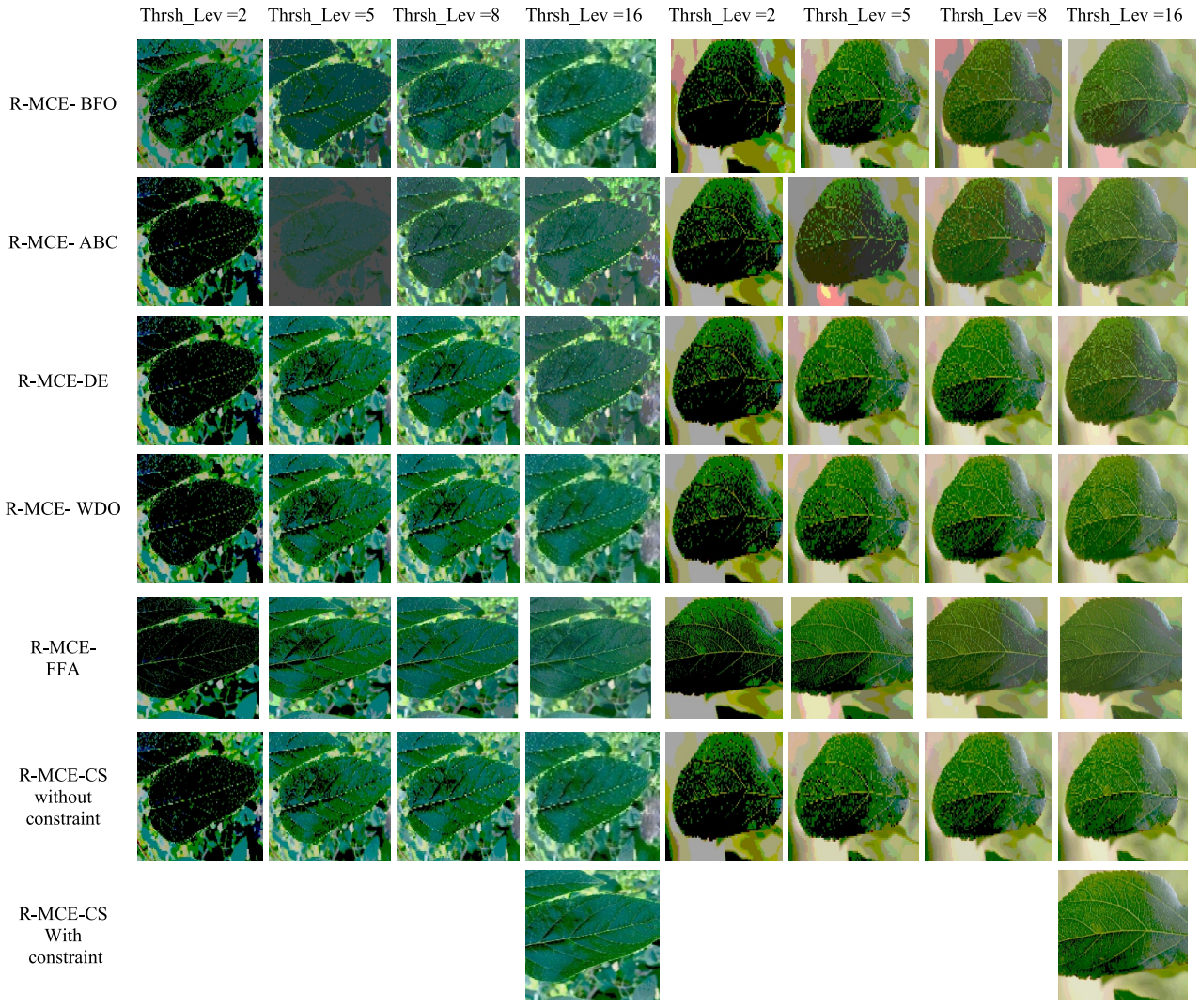

FIGURE 7 Segmented image of crop images (g) and (h) for level 16 based on the proposed technique and other algorithms for levels 2, 5, 8, and 16

17519683, 2022, 6, Downloaded from https://ietresearch.onlinelibrary.wiley.com/doi/10.1049/ipr2.12148 by Gwangju Institute of Science and Technology (GIST), Wiley Online Library on [05/09/2024]. See the Terms and Conditions (https://onlinelibrary.wiley.com/terms-and-conditions) on Wiley Online Library for rules of use; OA articles are governed by the applicable Creative Commons License

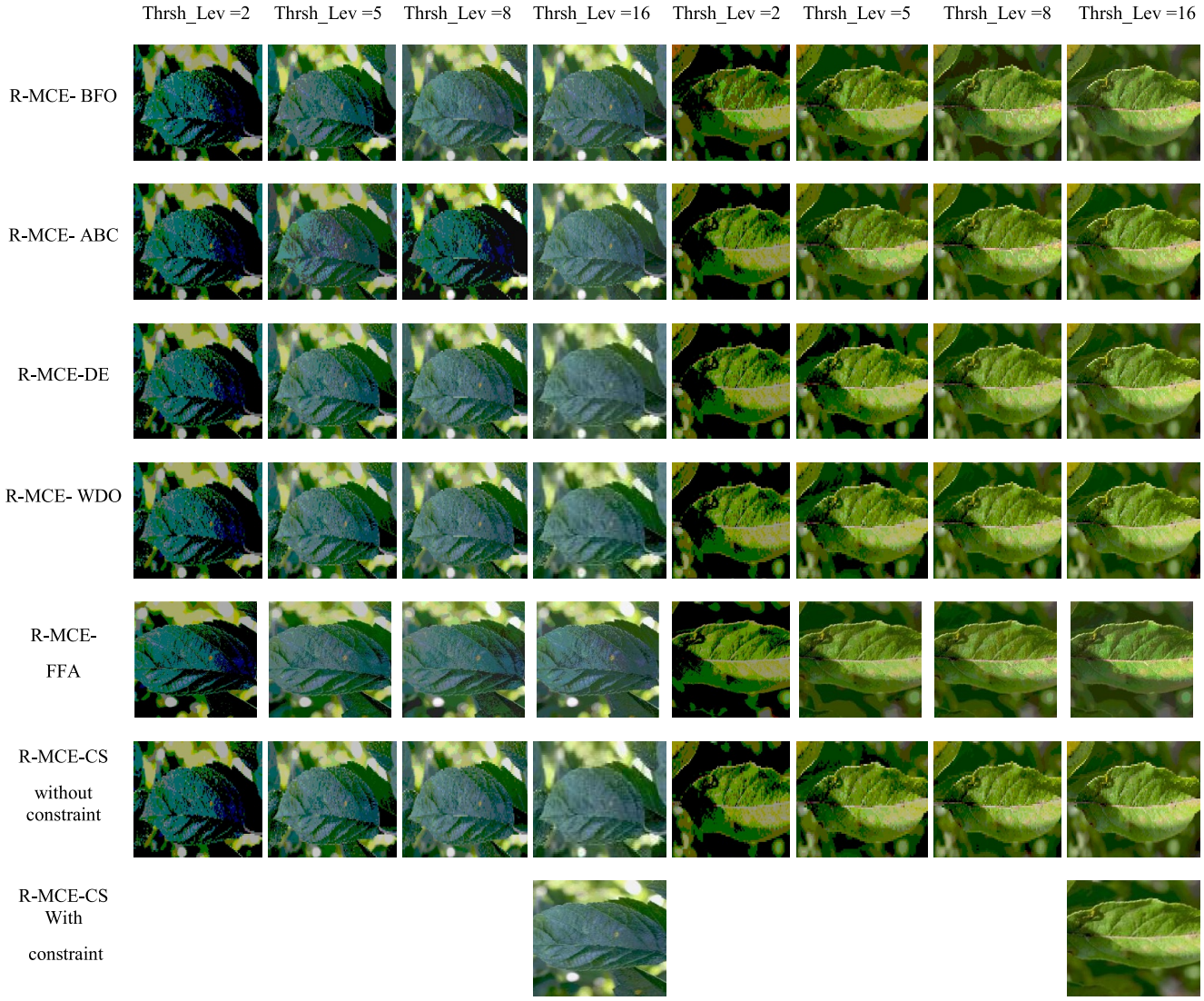

FIGURE 8 Segmented image of crop images (i) and (j) for level 16 based on the proposed technique and other algorithms for levels 2, 5, 8 and 16

of pixel) with multiple peaks and valleys. The size of the image is 2048 × 1365 with a bit depth of 24 and is taken from Refs. [10, 11]. The nature of these images is highly dense. Therefore, the MLT of such types of crop images is a challenging task.

In this paper, recursive minimum cross entropy (R-MCE) and CS algorithm have been combined for MLT of crop images. This technique (R-MCE-CS) finds the optimal threshold value efficiently by minimising the cross entropy between the original and segmented image. This technique reduces the complexity of computation when it is used for MLT, but still, it is useful for bi-level thresholding. Hence, the CS algorithm has been combined with recursive minimum cross entropy (R-MCE) that efficiently searches the optimal threshold value and improves the accuracy. Lévy flight has been used for exploration, which resolves structural optimisation issues. This technique (R-MCE-CS) has been compared with the well-known optimisation algorithm shown in Figures 4–8 which show a better result qualitatively. This proposed method uses one constraint on the SSIM, which leads to an increment in the accuracy for a higher thresholding level. The accuracy of the proposed technique has been evaluated on 10 crop images with complex backgrounds and different illumination of colour intensity space. The result has been confirmed qualitatively and quantitively, which is used to demonstrate the utility of the proposed method.

There are several parameter values used during this experiment and the best values are selected, as shown in Table 1. The evaluation parameters such as mean square error (MSE), peak signal to noise ratio (PSNR), SSIM, and feature similarity index (FSIM) have been used to investigate the performance of the proposed algorithm.

5.1 | Performance evaluation

Under this section, some important performance evaluation parameters such as PSNR, MSE, SSIM, and FSIM have been used to demonstrate the comparison of the algorithm. The

17519683, 2022, 6, Downloaded from https://ietresearch.onlinelibrary.wiley.com/doi/10.1049/ipr2.12148 by Gwangju Institute of Science and Technology (GIST), Wiley Online Library on [05/09/2024]. See the Terms and Conditions (https://onlinelibrary.wiley.com/terms-and-conditions) on Wiley Online Library for rules of use; OA articles are governed by the applicable Creative Commons License

fidelity parameter confirms the accuracy and quality of the outcome image, which is defined as follows:

5.1.1 | MSE

The MSE is used to calculate the error between the segmented image I_{segmt} and the original image I_{orgnl} of size $M \times N$. A lower value of mean square error indicates a good sign of segmentation.

$$\mathrm{MSE} = \frac{1}{M \times N} \sum_{i=1}^{M} \sum_{i=1}^{N} \left[I_{orgnl}(i,j) - I_{segmt}(i,j) \right]^2 \tag{16}$$

5.1.2 | PSNR

The PSNR is an evaluation matrix that is utilised to measure image quality. A higher value of PSNR indicates a good sign of segmentation [3, 26].

$$\mathrm{PSNR} = 10 \log 10 \left(\frac{(255)^2}{\mathrm{MSE}} \right) \tag{17}$$

5.1.3 | SSIM

The SSIM is used to measure the structural similitude between the segmented and the original image. It is defined under Section 2.2.

5.1.4 | FSIM

The FSIM is used for mapping the feature and utilised for similarity measurement of the original and outcome image [3, 26].

$$\mathrm{FSIM}\left(I_{orgnl}, I_{segmt}\right) = \frac{\sum_{X \in \Omega} PCm(X) \times SL(X)}{\sum_{X \in \Omega} PCm(X)} \tag{18}$$

In Equation (18), X represents the whole image domain. $S_L(X)$ represents the similitude between I_{orgnl} and I_{segmt}. PC_m represents the phase consistency of segmented and original images, respectively. For the RGB image, it is represented as:

$$\mathrm{FSIM} = \sum_{c} \mathrm{FSIM}\left(I^{c}_{orgnl}, I^{c}_{segmt} \right) \tag{19}$$

5.2 | Experimental result analysis without constraint using R-MCE-CS

In this experiment, R-MCE has been used as an objective function to choose the optimal threshold value by minimising the cross entropy between the object of interest and background. The computational effort of computing gets reduced by using recursive programming for MLT [34, 49], but still, it is

TABLE 1 Parameter's value used in different algorithms

Algorithms	Parameter	Value
BFO	Number of bacterium	25
	Chemotactic steps	10
	Reproduction steps count	10
	No. of eliminations of a dispersal event	10
	Depth of attractant	0.1
	Elimination and dispersal's probability	0.9
	Height of repellent	0.1
	Width of repellent	10
	Swimming length	10
	Width of attractant	0.2
DE	Total iterations	300
	Population	25
	Crossover probability	0.2
	Scaling factor	0.5
CS	Total nests	25
	Scaling factor	1.5
	Total iterations	300
	Probability of mutation	0.25
ABC	Swarm size	25
	Maximum trial limit	10
	Total iterations	300
	Lower bound	1
	Upper bound	256
	Value of $F_i(\varphi)$	0 1
FFA	Number of fireflies	25
	Light absorption coefficient at the source	1
	Size of initial firefly	25
	Randomisation parameter	0.5
	Maximum iteration number	300
	Inertial attractiveness	0.2
WDO	Maximum number of iterations	300
	Population	25
	Gravitational constant	0.2
	Coriolis effect coefficient	0.4
	Velocity limit	0.2
	RT coefficient	3
	Constant in update equation	0.4

17519683, 2022, 6, Downloaded from https://ietresearch.onlinelibrary.wiley.com/doi/10.1049/ipr2.12148 by Gwangju Institute of Science and Technology (GIST), Wiley Online Library on [05/09/2024]. See the Terms and Conditions (https://onlinelibrary.wiley.com/terms-and-conditions) on Wiley Online Library for rules of use; OA articles are governed by the applicable Creative Commons License

TABLE 2 Comparative analysis of different algorithms for PSNR evaluated using recursive MCE

Original crop images	Level	BFO PSNR	ABC PSNR	DE PSNR	WDO PSNR	FFA PSNR	Proposed method without constraint PSNR	Proposed method with constraint PSNR
a	2	14.3472	14.5354	13.9598	**14.6523**	14.3472	**14.6523**	
	5	16.9741	18.1799	18.1775	19.1190	16.9741	**20.3363**	
	8	20.8690	19.9391	20.7018	21.4699	20.8690	**21.4858**	
	16	23.0684	25.2920	23.9259	24.4467	23.0684	26.1163	**26.1303**
b	2	12.2178	13.6747	**13.6756**	13.6747	12.2178	**13.6756**	
	5	16.8274	19.5844	18.1795	**19.6824**	16.8274	19.5340	
	8	21.1836	20.7015	20.5438	**23.0824**	21.1836	23.0284	
	16	24.1488	25.1381	28.1840	28.1820	24.1488	29.5889	**29.6188**
c	2	13.2646	13.6177	13.9093	13.9026	13.2646	**13.9598**	
	5	17.4166	17.0724	17.7794	17.5690	17.4166	**17.9768**	
	8	20.3569	18.4809	20.4191	20.4142	20.3569	**20.7240**	
	16	21.6506	24.0635	24.4954	24.0831	21.6506	**25.9795**	24.4783
d	2	14.5696	14.8599	14.9456	**14.9487**	14.5696	14.9456	
	5	16.7334	19.5759	20.2616	19.9569	16.7334	**20.3140**	
	8	22.1653	22.5952	23.0846	22.5712	22.1653	**23.1137**	
	16	26.7473	26.3440	27.6233	26.0310	26.7473	27.9514	**27.9607**
e	2	11.1160	13.5548	**13.7988**	**13.7988**	11.1160	**13.7988**	
	5	18.0102	18.2476	18.1732	18.1834	18.0102	**18.2885**	
	8	20.4656	20.2322	20.1187	20.0307	20.4656	**20.4935**	
	16	22.4204	22.4590	24.6069	23.5942	22.4204	25.1854	**27.7125**
f	2	12.2722	9.8656	**12.5906**	12.4972	12.2700	**12.5906**	
	5	16.7019	17.0767	17.4044	17.2589	16.7000	**17.4049**	
	8	18.7795	18.2111	19.9975	20.2085	18.7800	**20.3770**	
	16	25.8778	22.3669	26.2449	25.7089	25.8800	27.1341	**27.2406**
g	2	9.9468	10.6232	**10.6840**	10.6834	9.9500	**10.6840**	
	5	13.5881	14.5911	15.5051	15.115	13.5900	**15.5252**	
	8	15.7049	15.0823	17.3423	16.9345	15.7000	**17.4296**	
	16	19.9127	20.3954	19.1773	20.7563	19.9100	**21.6370**	20.7200
h	2	11.2480	12.1751	**12.3393**	12.3313	11.2500	**12.3393**	
	5	15.4563	15.4299	15.2070	15.3843	15.4600	**15.5386**	
	8	16.0351	16.6202	17.2697	17.4876	16.0400	**17.5081**	
	16	20.0277	19.6512	20.0876	20.4789	20.0300	20.6135	**20.6140**
i	2	11.7104	11.9109	**12.1545**	12.1497	11.7100	**12.1545**	
	5	15.7333	16.3467	17.1915	17.1928	15.7300	**17.4092**	
	8	18.4732	19.3682	20.4508	20.8278	18.4700	**20.9081**	
	16	23.8002	27.4860	25.1215	22.2282	23.8000	**28.3810**	25.4625
j	2	12.5651	13.1764	13.9598	13.8916	12.5700	**14.4073**	
	5	18.5735	16.7873	17.9768	17.7376	18.5700	**19.1897**	
	8	20.9962	20.2006	20.5131	20.5276	21.1200	**21.1640**	
	16	23.3300	22.6674	24.6809	23.1149	23.3300	24.7688	**25.3581**

Note: Bold values signify the best fidelity parameter obtained

17519683, 2022, 6, Downloaded from https://ietresearch.onlinelibrary.wiley.com/doi/10.1049/ipr2.12148 by Gwangju Institute of Science and Technology (GIST), Wiley Online Library on [05/09/2024]. See the Terms and Conditions (https://onlinelibrary.wiley.com/terms-and-conditions) on Wiley Online Library for rules of use; OA articles are governed by the applicable Creative Commons License

TABLE 3 Comparative analysis of different algorithms for MSE evaluated using recursive MCE

Original crop images	Level	BFO MSE	ABC MSE	DE MSE	WDO MSE	FFA MSE	Proposed method without constraint MSE	Proposed method with constraint MSE
a	2	2398.3618	2295.6793	2707.1156	**2235.0012**	2398.3618	**2235.0012**	
	5	1307.4189	995.2618	1032.8773	811.3278	1307.4189	**622.7123**	
	8	550.1470	682.1414	636.9763	497.1343	550.1470	**495.6559**	
	16	343.8214	202.3548	351.8111	287.5395	343.8214	196.6104	**196.2852**
b	2	3924.5777	2797.4194	**2797.2759**	2797.4194	3924.5777	**2797.2759**	
	5	1370.0697	729.8936	1032.5462	**717.6252**	1370.0697	744.3756	
	8	495.5332	571.0640	661.4929	**336.8841**	495.5332	338.8331	
	16	261.0380	202.0480	109.0140	105.1918	261.0380	72.0437	**71.7178**
c	2	3066.5656	2830.1945	**2648.6268**	2652.6575	3066.5656	2707.1156	
	5	1181.4965	1277.4016	1084.3736	1138.1914	1181.4965	**1076.2749**	
	8	618.6237	924.7729	**618.2236**	618.7788	618.6237	635.1739	
	16	449.5698	256.7563	294.7254	316.9548	449.5698	**227.0799**	295.1761
d	2	2289.6680	2163.2706	2123.3315	**2120.6359**	2289.6680	2123.3315	
	5	1389.5095	720.0121	613.3301	657.9991	1389.5095	**606.1295**	
	8	401.5253	358.1143	320.5345	364.6930	401.5253	**318.3679**	
	16	142.2422	152.1944	115.2048	170.9247	142.2422	105.7208	**105.5670**
e	2	5075.6011	2877.1623	**2718.3446**	**2718.3446**	5075.6011	**2718.3446**	
	5	1029.2688	985.2834	1005.0257	1001.5439	1029.2688	**979.1592**	
	8	**584.6886**	617.2254	660.9374	673.1539	**584.6886**	611.2078	
	16	392.1717	375.1120	278.3642	339.2449	392.1717	258.7519	**119.9728**
f	2	**2398.3618**	6712.4828	3635.9231	3711.9387	3891.3000	3635.9231	
	5	1307.4189	**1276.5468**	1289.9843	1331.9862	1417.1400	1290.116	
	8	**550.1470**	998.7953	751.5391	722.1352	942.9300	693.6849	
	16	343.8214	377.5597	181.6948	220.4210	168.3400	147.8663	**142.6493**
g	2	**3891.30**	5747.0567	5663.3194	5664.1283	6749.5100	5663.3194	
	5	**1417.14**	2296.5141	2019.1883	2174.8743	2931.7100	2015.3931	
	8	**942.93**	2147.3315	1477.2729	1591.2679	1756.6700	1466.3369	
	16	**759.3304**	889.3177	1144.5751	859.5986	779.4400	779.0304	918.7797
h	2	6749.51	3942.9108	**3799.5820**	3806.8248	4890.1300	**3799.5820**	
	5	2931.71	1896.2517	2017.8551	1944.9409	1916.1600	**1885.0469**	
	8	1756.67	1460.9533	1333.0515	1279.3078	1695.8300	**1273.4754**	
	16	759.44	750.8436	648.22960	778.2336	646.2600	765.6803	**644.1502**
i	2	4890.13	4196.8556	**3967.5816**	3972.2098	4398.0500	**3967.5816**	
	5	1916.16	1521.4086	1307.9511	1307.7845	1779.5400	**1249.3665**	
	8	1695.83	836.5998	662.5620	600.3443	994.6300	**593.9324**	
	16	646.26	116.5757	247.0123	478.8115	275.0100	**95.99040**	226.5226
j	2	4398.05	3272.0907	2707.1156	2753.2739	3832.5800	**2423.7906**	
	5	1779.54	1382.5433	1076.2749	1128.9107	937.4300	**823.4593**	
	8	994.63	681.8859	663.7760	662.4808	**517.9500**	567.4308	
	16	275.01	426.3925	288.4238	420.9683	320.0800	304.3134	**269.6546**

Note: Bold values signify the best fidelity parameter obtained

17519683, 2022, 6, Downloaded from https://ietresearch.onlinelibrary.wiley.com/doi/10.1049/ipr2.12148 by Gwangju Institute of Science and Technology (GIST), Wiley Online Library on [05/09/2024]. See the Terms and Conditions (https://onlinelibrary.wiley.com/terms-and-conditions) on Wiley Online Library for rules of use; OA articles are governed by the applicable Creative Commons License

useful for bi-level thresholding. Hence, the CS via Lévy flight has been combined with recursive minimum cross entropy to increase the accuracy. This method efficiently searches the optimal threshold value for MLT. The multilevel segmentation of crop images has been compared with another five meta-heuristic optimisation algorithms such as DE, BFO, ABC, WDO, and FFA. The simulation results show a better visual result of a segmented image shown in Figures 4–8. The experimental result has been processed 10 times for each cropped image to avoid discrepancy.

Tables 2 and 3 illustrate the quantitative results of PSNR and MSE for different levels of thresholding (2, 5, 8 and 16). A higher PSNR and lower value of MSE indicate a good sign of segmentation. The R-MCE-CS shows a better value of PSNR than the other five existing algorithms such as WDO, ABC, BFO, DE, and FFA. The accuracy of the algorithm is validated using PSNR and MSE values. The comparative results of PSNR and MSE have been shown in Figures 9 and 10 for different levels of thresholding (2, 5, 8, and 16). In Figures 9 and 10 different notation has been used to represent the MLT of 10 crop images. $A_2(level = 2)$, $A_5(level = 5)$, $A_8(level = 8)$, and $A_{16}(level = 16)$ represent the four thresholding levels for first crop images, and $B_2(level = 2)$, $B_5(level = 5)$, $B_8(level = 8)$, and $B_{16}(level = 16)$ represent the four thresholding levels for second crop images. Likewise, C to J have been used for the rest of the eight crop images at a different level of thresholding. Figures 9 and 10 validate the accuracy of the algorithm.

Tables 4 and 5 illustrate the SSIM and FSIM values for different levels of thresholding (2, 5, 8 and 16). The best value of SSIM and FSIM is selected out of all values. A higher SSIM value indicates better segmentation. The R-MCE-CS shows a better result of SSIM than the other five existing algorithms such as WDO, ABC, BFO, DE, and FFA. The comparative results of SSIM and MSIM have been shown for different levels of thresholding (2, 5, 8 and 16) in Figures 11 and 12. In Figures 11 and 12, a different notation has been used to represent the MLT of 10 crop images. $A_2(level = 2)$, $A_5(level = 5)$, $A_8(level = 8)$, and $A_{16}(level = 16)$ represent the four thresholding levels for first crop images and $B_2(level = 2)$, $B_5(level = 5)$, $B_8(level = 8)$, and $B_{16}(level = 16)$ represent the four thresholding levels for second crop images. Likewise, C to J have been used for the rest of the eight crop images at a different level of thresholding. Figures 11 and 12 validate the accuracy of the segmented image. Because real-time applications require less processing time while maintaining high performance. Each algorithm's time complexity (CPU time) has been assessed and listed in Table 6. The CPU time required for the CS algorithm using recursive minimum cross entropy increases as the number of threshold levels increases, but it is found to be less than that for other algorithms such as WDO, ABC, BFO, DE, and FFA. The R-MCE-DE and R-MCE-CS are comparable for a few cases at the lower level of thresholding, $level = 2$, as shown in Tables 2–5. A few cases for a lower level of segmentation, DE algorithm, and WDO give almost similar results. The R-MCE-CS shows better outcome images than the other five existing algorithms such as BFO, ABC, WDO DE, and FFA.

5.3 | Experimental result analysis with constraint on SSIM using R-MCE-CS

Under Section 5.2, we have used a CS algorithm via Lévy flight and combined it with R-MCE. This technique efficiently searches the optimal threshold value by minimising the cross entropy between the original and the outcome image. Lévy flights have been used due to their good exploration capability.

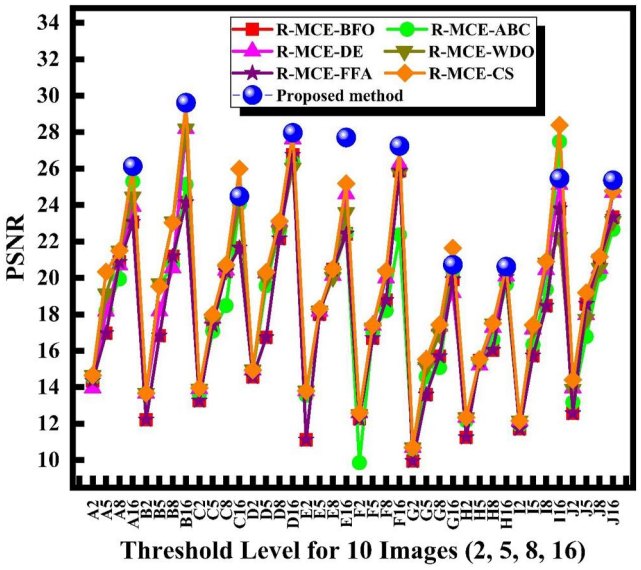

FIGURE 9 PSNR comparison using recursive MCE for different algorithms and the proposed method

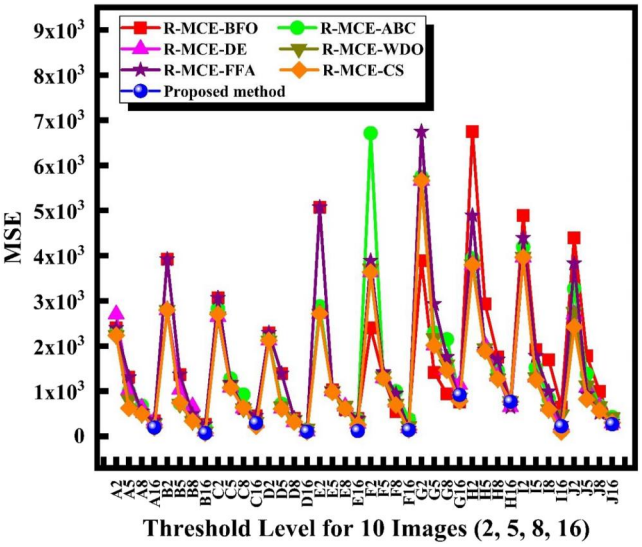

FIGURE 10 MSE comparison using recursive MCE for different algorithms and the proposed method

17519683, 2022, 6, Downloaded from https://ietresearch.onlinelibrary.wiley.com/doi/10.1049/sil2.12148 by Gwangju Institute of Science and Technology (GIST), Wiley Online Library on [05/09/2024]. See the Terms and Conditions (https://onlinelibrary.wiley.com/terms-and-conditions) on Wiley Online Library for rules of use; OA articles are governed by the applicable Creative Commons License

TABLE 4 Comparative analysis of different algorithms for SSIM evaluated using recursive MCE

Original crop images	Level	BFO SSIM	ABC SSIM	DE SSIM	WDO SSIM	FFA SSIM	Proposed method without constraint SSIM	Proposed method with constraint SSIM
a	2	0.9219	0.9253	0.9112	**0.9274**	0.9219	**0.9274**	
	5	**0.9857**	0.9658	0.9634	0.9715	**0.9857**	0.9780	
	8	0.9806	0.9754	0.9764	0.9818	0.9806	**0.9819**	
	16	0.9877	**0.9928**	0.9864	0.9889	0.9877	0.9926	0.9926
b	2	0.8829	0.9141	**0.9142**	0.9141	0.8829	**0.9142**	
	5	0.9634	0.9766	0.9634	**0.9772**	0.9634	0.9762	
	8	0.9863	0.9811	0.9755	0.9890	0.9863	**0.9892**	
	16	0.9917	0.9950	0.9962	0.9965	0.9917	**0.9981**	**0.9981**
c	2	0.9102	0.9162	**0.9222**	0.9221	0.9102	0.9112	
	5	**0.9677**	0.9579	0.9643	0.9623	**0.9677**	0.9618	
	8	**0.9818**	0.9683	0.9785	0.9785	**0.9818**	0.9765	
	16	0.9869	**0.9930**	0.9890	0.9882	0.9869	0.9914	0.9890
d	2	0.9347	0.9366	0.9386	0.9386	0.9347	**0.9390**	
	5	0.9575	0.9771	0.9820	0.9803	0.9575	**0.9825**	
	8	0.9905	0.9889	0.9903	0.9880	**0.9905**	0.9904	
	16	**0.9966**	0.9951	0.9962	0.9939	**0.9966**	**0.9966**	**0.9966**
e	2	0.8619	0.9190	**0.9238**	**0.9238**	0.8619	**0.9238**	
	5	**0.9754**	0.9696	0.9681	0.9684	**0.9754**	0.9691	
	8	**0.9868**	0.9821	0.9777	0.9772	**0.9868**	0.9794	
	16	0.9883	0.9897	0.9901	0.9877	0.9883	0.9905	**0.9961**
f	2	0.8936	0.8297	**0.8968**	0.8947	0.8900	**0.8968**	
	5	0.9590	**0.9696**	0.9585	0.9573	0.9600	0.9585	
	8	0.9694	0.9727	0.9750	0.9757	0.9700	**0.9766**	
	16	0.9951	0.9907	0.9940	0.9924	0.9935	**0.9957**	0.9953
g	2	0.8050	0.8290	**0.8311**	**0.8311**	0.8100	**0.8311**	
	5	0.9044	**0.9368**	0.9325	0.9276	0.9000	0.9325	
	8	**0.9518**	0.9405	0.9488	0.9450	0.9500	0.9489	
	16	0.9747	0.9678	0.9588	0.9689	0.9700	0.9714	**0.9964**
h	2	0.8614	0.8853	**0.8901**	0.8900	0.8600	**0.8901**	
	5	0.9397	**0.9575**	0.9352	0.9372	0.9400	0.9391	
	8	0.9449	**0.9646**	0.9549	0.9372	0.9400	0.9568	
	16	0.9820	0.9869	**0.9883**	0.9724	0.9800	0.9725	0.9725
i	2	0.8669	0.8717	**0.8783**	**0.8783**	0.8700	**0.8783**	
	5	0.9407	0.9553	0.9570	0.9570	0.9400	**0.9587**	
	8	0.9667	0.9706	0.9773	**0.9798**	0.9700	0.9796	
	16	0.9916	0.9966	0.9910	0.9826	0.9900	**0.9973**	0.9918
j	2	0.8806	0.8927	0.9112	0.9097	0.8800	**0.9209**	
	5	0.9675	0.9505	0.9618	0.9599	0.9700	**0.9715**	
	8	**0.9829**	0.9753	0.9755	0.9755	0.9800	0.9792	
	16	0.9888	0.9840	0.9891	0.9838	0.9800	**0.9892**	**0.9896**

Note: Bold values signify the best fidelity parameter obtained

17519683, 2022, 6, Downloaded from https://ietresearch.onlinelibrary.wiley.com/doi/10.1049/ipr2.12148 by Gwangju Institute of Science and Technology (GIST), Wiley Online Library on [05/09/2024]. See the Terms and Conditions (https://onlinelibrary.wiley.com/terms-and-conditions) on Wiley Online Library for rules of use; OA articles are governed by the applicable Creative Commons License

TABLE 5 Comparative analysis of different algorithms for FSIM evaluated using recursive MCE

Original crop images	Level	BFO FSIM	ABC FSIM	DE FSIM	WDO FSIM	FFA FSIM	Proposed method without constraint FSIM	Proposed method with constraint FSIM
a	2	0.7185	0.7205	**0.7274**	0.7217	0.7185	0.7217	
	5	0.8244	0.8087	0.8011	0.8319	0.8244	**0.8536**	
	8	0.8599	0.8496	0.8564	0.8820	0.8599	**0.8826**	
	16	0.9013	0.9182	0.9083	0.9239	0.9013	**0.9381**	**0.9390**
b	2	0.6614	0.6698	**0.6706**	0.6698	0.6614	**0.6706**	
	5	0.7334	0.7968	0.8011	0.8103	0.7334	**0.8123**	
	8	0.7959	0.8266	0.8579	0.8824	0.7959	**0.8860**	
	16	0.8710	0.8672	0.9346	0.9455	0.8710	**0.9618**	0.9610
c	2	0.6977	0.6985	0.7001	0.6999	0.6977	**0.7274**	
	5	0.7590	0.7862	0.7893	0.7889	0.7590	**0.8003**	
	8	0.8259	0.8185	0.8518	0.8513	0.8259	**0.8591**	
	16	0.8505	0.8731	**0.9281**	0.9209	0.8505	0.9193	0.9279
d	2	0.6875	0.7120	0.7126	**0.7130**	0.6875	0.7126	
	5	0.7576	0.8544	**0.8639**	0.8572	0.7576	**0.8639**	
	8	0.8835	0.9072	0.9180	0.9147	0.8835	**0.9194**	
	16	0.9422	0.9576	0.9687	0.9525	0.9422	0.9694	**0.9698**
e	2	0.6415	0.6816	**0.6848**	**0.6848**	0.6415	**0.6848**	
	5	0.7736	0.8023	0.8103	0.8118	0.7736	**0.8120**	
	8	0.8049	0.8297	0.8622	0.8673	0.8049	**0.8705**	
	16	0.8570	0.8470	0.9313	0.9273	0.8570	0.9423	**0.9566**
f	2	0.6424	0.5651	**0.6438**	0.6429	0.6400	**0.6438**	
	5	0.7523	0.7114	0.8025	0.8022	0.7500	**0.8030**	
	8	0.8164	0.7795	0.8711	0.8780	0.8200	**0.8808**	
	16	0.9080	0.8591	0.9539	0.9508	0.9100	0.9635	**0.9636**
g	2	0.6137	0.6584	0.6605	**0.6607**	0.6100	0.6605	
	5	0.7364	0.6617	0.7776	0.7716	0.7400	**0.7824**	
	8	0.7032	0.7342	0.8253	0.8235	0.7000	**0.8344**	
	16	0.8756	0.8876	0.8683	0.8871	0.8800	**0.9035**	0.8567
h	2	0.6813	0.6985	**0.7019**	**0.7019**	0.6800	**0.7019**	
	5	0.7599	0.7517	0.7589	0.7632	0.7600	**0.7643**	
	8	0.7655	0.7524	0.8009	0.7632	0.7700	**0.8072**	
	16	0.8283	0.8272	0.8302	0.8572	0.8300	0.8632	**0.8642**
i	2	0.6898	0.6900	0.6910	**0.6913**	0.6900	0.6910	
	5	0.7722	0.7649	0.8115	0.8095	0.7700	**0.8136**	
	8	0.8119	0.8522	0.8644	0.8666	0.8100	**0.8718**	
	16	0.8894	0.9362	0.9293	0.8999	0.8900	**0.9479**	0.9319
j	2	0.6973	0.7090	0.7274	0.7270	0.7000	**0.7277**	
	5	0.7956	0.7947	0.8003	0.7972	0.8000	**0.8098**	
	8	0.8250	0.8402	0.8583	0.8583	0.8300	**0.8614**	
	16	0.8704	0.8818	0.9057	0.9015	0.8700	0.9211	**0.9245**

Note: Bold values signify the best fidelity parameter obtained

17519683, 2022, 6, Downloaded from https://ietresearch.onlinelibrary.wiley.com/doi/10.1049/ipr2.12148 by Gwangju Institute of Science and Technology (GIST), Wiley Online Library on [05/09/2024]. See the Terms and Conditions (https://onlinelibrary.wiley.com/terms-and-conditions) on Wiley Online Library for rules of use; OA articles are governed by the applicable Creative Commons License

But we aim to improve the accuracy of the segmented image. Hence, one constraint has been applied to SSIM described in the flow chart of the proposed method, which leads to an increment in the accuracy for a higher thresholding level. This simulation has been evaluated on 10 different complex background crop images with a high dimension of colour intensity space.

Tables 2 and 3 illustrate the quantitative results of PSNR and MSE for higher levels of thresholding (level = 16). A higher PSNR and lower value of MSE indicate a good sign of segmentation. The simulation result evidences that the proposed technique shows a better value of PSNR and MSE for seven crop images out of 10. The comparative results of PSNR and MSE have been shown in Figures 9 and 10, which validate the accuracy of the algorithms. The notation for Figures 9–12 has been described under Section 5.2 to denote the different level thresholding of 10 crop images.

Tables 4 and 5 illustrate the quantitative results of SSIM and FSIM values for higher levels of thresholding (level = 16). The best result of SSIM and FSIM have been selected. A higher value of SSIM (tends towards 1) indicates the better accuracy of the segmented image. The simulation result evidences that the proposed technique using constraint on SSIM shows improvement in accuracy. The comparative results of SSIM and FSIM have been depicted in Figures 11 and 12, which validate the high quality of the outcome image. The time complexity is depicted in Table 6. In comparison to R-MCE-CS discussed under Section 5.2, it gives a comparable performance in terms of CPU time for a higher thresholding level. However, the accuracy of the segmented image has been improved in terms of fidelity parameters.

6 | CONCLUSION

In this paper, the R-MCE technique has been applied for multilevel thresholding (MLT) of crop images. The R-MCE technique is not sufficient to choose optimal threshold values efficiently. Therefore, the CS algorithm with Lévy flights has been incorporated with R-MCE to increase the accuracy. Lévy flights have good exploration capability due to random walks. The simulation results evidence that the proposed technique without constraint (R-MCE-CS) produces an improvement in accuracy than the existing algorithms in terms of MSE, PSNR, SSIM, and FSIM, at various levels of thresholding. Because real-time applications require less processing time while maintaining high performance, which is validated by the CS algorithm using recursive minimum cross entropy (R-MCE-CS) without constraint. Secondly, in the proposed method, one constraint has been applied to the SSIM, which leads to an improvement in the accuracy for a higher level of thresholding. This leads to an extra benefit in terms of fidelity parameters. The improvement in accuracy is the major strength of the proposed method. This technique takes almost equal or little more when it is applied for a lower level of thresholding. The quantitative and qualitative results show that the proposed technique produces a high quality of segmented images across 10 different complex background crop images and a high dimension of colour intensity space. The objective of this paper is not to create an MLT algorithm that can beat all currently known techniques but to highlight the histogram-based MLT, which can be a worthwhile option for crop image segmentation. As a promising result of the proposed method, it can be used in other applications of image processing, such as image enhancement and image classification, etc. Furthermore, this technique can be applied in the segmentation of medical images for diagnosis purposes. In future, the implementation of R-MCE-CS with an energy curve can be used for MLT of crop images.

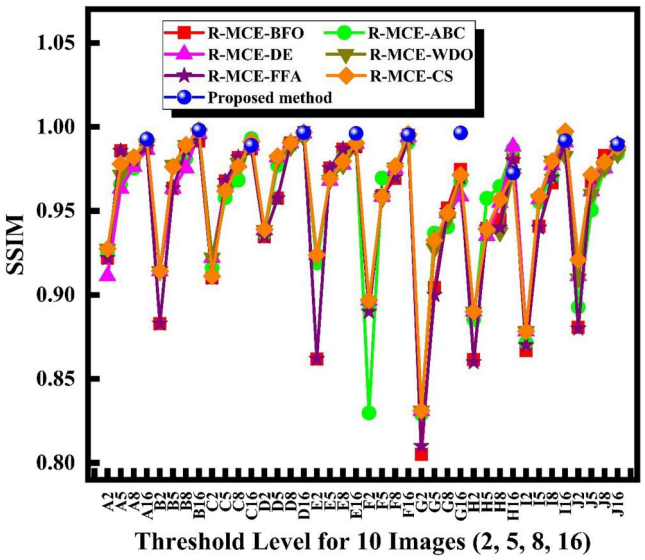

FIGURE 11 SSIM comparison using recursive MCE for different algorithms and the proposed method

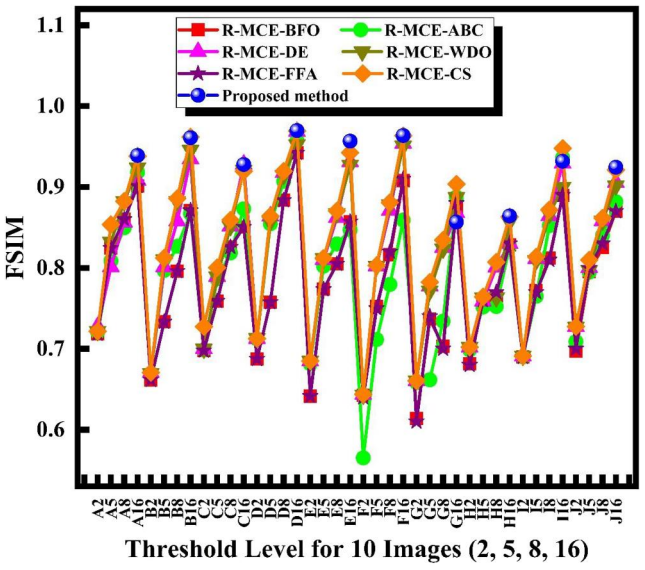

FIGURE 12 FSIM comparison using recursive MCE for different algorithms and the proposed method

17519683, 2022, 6, Downloaded from https://ietresearch.onlinelibrary.wiley.com/doi/10.1049/sil2.12148 by Gwangju Institute of Science and Technology (GIST), Wiley Online Library on [05/09/2024]. See the Terms and Conditions (https://onlinelibrary.wiley.com/terms-and-conditions) on Wiley Online Library for rules of use; OA articles are governed by the applicable Creative Commons License

TABLE 6 Comparative analysis of different algorithms for CPU time evaluated using recursive MCE

Original crop images	Level	BFO CPU time	ABC CPU time	DE CPU time	WDO CPU time	FFA CPU time	Proposed method without constraint CPU time	Proposed method with constraint CPU time
a	2	19.1859	11.5038	10.5137	11.3968	10.1746	**9.5832**	
	5	23.2861	12.2856	11.1479	11.7284	10.9299	**9.9594**	
	8	27.4088	12.8587	11.4414	12.4232	11.5618	**10.3330**	
	16	33.3387	14.6579	11.6389	14.9520	12.3744	**11.5529**	12.9416
b	2	19.0018	11.6568	10.3321	11.3400	11.3350	**9.5754**	
	5	21.9509	12.4851	10.9205	11.7082	11.7737	**9.8715**	
	8	26.4872	12.9456	11.1672	12.6602	12.3282	**10.1799**	
	16	36.1283	13.9491	11.0005	14.7748	15.5389	**10.3583**	11.4617
c	2	19.2191	11.9798	10.4952	11.8525	11.4927	**9.5666**	
	5	24.3863	12.4906	11.0433	12.6238	11.7472	**9.9218**	
	8	26.9612	12.6179	11.5259	12.8077	12.1094	**10.4705**	
	16	34.9549	13.6228	12.2592	15.4794	12.2768	**10.9504**	11.0966
d	2	18.9379	11.8854	10.5757	11.9139	11.3855	**9.5200**	
	5	23.7553	12.4610	10.9976	12.5438	11.6661	**9.9542**	
	8	26.0843	12.9181	11.5408	12.8928	12.3662	**10.5316**	
	16	36.8517	14.0961	12.4863	15.9679	12.8265	**11.5401**	12.2395
e	2	19.5287	11.8606	10.6282	11.9301	11.2169	**9.8547**	
	5	23.3897	12.0092	10.7940	11.6452	11.2875	**10.0852**	
	8	26.1949	12.2812	10.9104	12.5672	11.8618	**10.3477**	
	16	32.0195	13.6231	12.2277	16.2015	12.0573	**11.1136**	12.1687
f	2	19.5355	11.8184	10.5845	11.6884	10.9786	**9.4923**	
	5	25.1727	12.4871	10.6857	13.0995	11.9194	**9.7610**	
	8	26.7503	12.9536	10.7154	13.5993	12.0292	**10.5230**	
	16	33.2339	13.3025	11.5290	14.1378	12.9819	**10.7021**	10.8528
g	2	19.6200	11.7775	10.5025	11.7867	11.2110	**9.4924**	
	5	24.1866	12.4000	11.1989	12.3047	11.8070	**9.9974**	
	8	26.8006	12.7452	11.4920	12.6960	12.3203	**10.4285**	
	16	38.8058	14.6649	12.9957	15.9358	13.4858	**11.7235**	12.7979
h	2	20.9287	12.3799	11.4169	12.5308	10.1372	**9.1450**	
	5	25.0666	13.2012	11.7629	14.0388	12.0697	**10.5840**	
	8	30.3928	13.5651	12.0263	14.0549	12.3089	**11.3694**	
	16	41.7574	15.8473	12.3041	18.0159	13.2466	**11.7779**	12.7404
i	2	20.2318	11.8702	10.6801	11.7547	11.4742	**9.9461**	
	5	24.9627	12.4999	11.2383	12.4081	11.7646	**10.3987**	
	8	25.6735	13.0836	11.4911	12.7719	12.0080	**10.6796**	
	16	36.2555	13.9486	13.3326	16.2574	13.1755	**12.9332**	13.3170
j	2	20.5287	11.7511	10.4974	11.6033	10.9931	**10.0149**	
	5	22.4561	12.4646	10.9094	12.1175	11.3008	**10.1045**	
	8	24.1357	12.9002	11.3933	12.3973	11.9898	**10.6781**	
	16	32.7706	13.8051	12.8666	15.5389	12.8054	**11.1921**	15.8903

Note: Bold values signify the best fidelity parameter obtained

17519683, 2022, 6, Downloaded from https://ietresearch.onlinelibrary.wiley.com/doi/10.1049/ipr2.12148 by Gwangju Institute of Science and Technology (GIST), Wiley Online Library on [05/09/2024]. See the Terms and Conditions (https://onlinelibrary.wiley.com/terms-and-conditions) on Wiley Online Library for rules of use; OA articles are governed by the applicable Creative Commons License

ACKNOWLEDGEMENT

There is no funding.

CONFLICT OF INTEREST

Authors have no conflict of interest.

DATA AVAILABILITY STATEMENT

The data used for this research work is available in Refs. [10, 11].

ORCID

Arun Kumar https://orcid.org/0000-0002-3945-4646

REFERENCES

1. He, L., Huang, S.: Modified firefly algorithm based multilevel thresholding for color image segmentation. Neurocomputing 240, 152–174 (2017). https://doi.org/10.1016/j.neucom.2017.02.040
2. Gao, R., Wu, H.: Agricultural image target segmentation based on fuzzy set. Optik 126(24), 5320–5324 (2015). https://doi.org/10.1016/j.ijleo.2015.09.006
3. Huang, Y.P., et al.: A type-2 fuzzy clustering and quantum optimization approach for crops image. Segmentation 23(3), 615–629 (2021). https://doi.org/10.1007/s40815-020-01009-2
4. Haug, S., Ostermann, J.: A crop/weed field image dataset for the evaluation of computer vision based precision agriculture tasks. Lect. Notes Comput. Sci. 8928, 105–116 (2014)
5. Lu, H., et al.: Joint crop and tassel segmentation in the wild. Proc. - 2015 Chinese Autom. Congr. CAC 2015, pp. 474–479 (2016)
6. Bhandari, A.K., et al.: A novel color image multilevel thresholding based segmentation using nature inspired optimization algorithms. Expert Syst. Appl. 63, 112–133 (2016). https://doi.org/10.1016/j.eswa.2016.06.044
7. Mukhopadhyay, S., et al.: Tea leaf disease detection using multi-objective image segmentation. Multimed. Tool. Appl. 80(1), 753–771 (2020). https://doi.org/10.1007/s11042-020-09567-1
8. Pare, S., et al.: Rényi's entropy and bat algorithm based color image multilevel thresholding. Adv. Intell. Syst. Comput. 748, 71–84 (2019)
9. Meyer, G.E., Hindman, T.W., Laksmi, K.: Machine vision detection parameters for plant species identification. Precision agriculture and biological quality 3543, 327–335 (1999)
10. Jiang, P., et al.: Real-time detection of apple leaf diseases using deep learning approach based on improved convolutional neural networks. IEEE Access 7, 59069–59080 (2019). https://doi.org/10.1109/access.2019.2914929
11. Luo, Y., et al.: Apple leaf disease recognition and sub-class categorization based on improved multi-scale feature fusion network. IEEE Access 9, 95517–95527 (2021). https://doi.org/10.1109/access.2021.3094802
12. Saŋ, T., Çunkaş, M.: Color image segmentation based on multiobjective artificial bee colony optimization. Appl. Soft Comput. 34, 389–401 (2015). https://doi.org/10.1016/j.asoc.2015.05.016
13. Feng, Y., et al.: Segmentation fusion based on neighboring information for MR brain images. Multimed. Tool. Appl. 76(22), 23139–23161 (2016). https://doi.org/10.1007/s11042-016-4098-3
14. Wang, C., et al.: A novel multi-scale segmentation algorithm for high resolution remote sensing images based on wavelet transform and improved JSEG algorithm. Optik 125(19), 5588–5595 (2014). https://doi.org/10.1016/j.ijleo.2014.07.002
15. Pare, S., et al.: Image segmentation using multilevel thresholding: a research review. Iran. J. Sci. Technol. Trans. Electr. Eng. 44(1), 1–29 (2019). https://doi.org/10.1007/s40998-019-00251-1
16. Bhandari, A.K., Singh, A., Kumar, I.V.: Spatial context energy curve-based multilevel 3-D Otsu algorithm for image segmentation. IEEE Trans. Syst. Man, Cybern. Syst. 51(5), 2760–2773 (2021). https://doi.org/10.1109/tsmc.2019.2916876
17. Pare, S., et al.: An optimal color image multilevel thresholding technique using grey-level co-occurrence matrix. Expert Syst. Appl. 87, 335–362 (2017). https://doi.org/10.1016/j.eswa.2017.06.021
18. Zahara, E., Fan, S.K.S., Tsai, D.M.: Optimal multi-thresholding using a hybrid optimization approach. Pattern Recogn. Lett. 26(8), 1082–1095 (2005). https://doi.org/10.1016/j.patrec.2004.10.003
19. Bai, X.D., et al.: Crop segmentation from images by morphology modeling in the CIE L*a*b* color space. Elsevier Enhanced Reader 99, 21–34 (2013). https://doi.org/10.1016/j.compag.2013.08.022
20. Wu, J., et al.: Automatic recognition of ripening tomatoes by combining multi-feature fusion with a Bi-layer classification strategy for harvesting robots. Sensors 19(3), 612 (2019). https://doi.org/10.3390/s19030612
21. Pare, S., et al.: A multilevel color image segmentation technique based on cuckoo search algorithm and energy curve. Allied Soft computing 47, 76–102 (2016). https://doi.org/10.1016/j.asoc.2016.05.040
22. Otsu, N.: A threshold selection method from gray-level histograms. IEEE Trans. Syst. Man. Cybern. 9(1), 62–66 (1979). https://doi.org/10.1109/tsmc.1979.4310076
23. Chaabane, S., Sayadi, M., , F.F-M.: Color image segmentation using automatic thresholding and the fuzzy C-means techniques. IEEE, 857–861 (2008)
24. Nandhini, S., et al.: Analysis on classification and prediction of leaf disease using deep neural network and image segmentation technique. Annals of the Romanian Society for Cell Biology 25, 9035–9041 (2021)
25. Pare, S., et al.: Backtracking search algorithm for color image multilevel thresholding. Signal, Image Video Process 12(2), 385–392 (2017). https://doi.org/10.1007/s11760-017-1170-z
26. Bhandari, A.K., Kumar, A., Singh, G.K.: Modified artificial bee colony based computationally efficient multilevel thresholding for satellite image segmentation using Kapur's, Otsu and Tsallis functions. Expert Syst. Appl. 42(3), 1573–1601 (2015). https://doi.org/10.1016/j.eswa.2014.09.049
27. Kandhway, P., Bhandari, A.K.: Spatial context-based optimal multilevel energy curve thresholding for image segmentation using soft computing techniques. Neural Comput. Appl. 32(13), 8901–8937 (2020). https://doi.org/10.1007/s00521-019-04381-9
28. Pare, S., et al.: A new technique for multilevel color image thresholding based on modified fuzzy entropy and Lévy flight firefly algorithm. Comput. Electr. Eng. 70, 476–495 (2018). https://doi.org/10.1016/j.compeleceng.2017.08.008
29. Bhandari, A.K.: A novel beta differential evolution algorithm-based fast multilevel thresholding for color image segmentation. Neural Comput. Appl. 32(9), 4583–4613 (2020). https://doi.org/10.1007/s00521-018-3771-z
30. Portes de Albuquerque, M., et al.: Image thresholding using Tsallis entropy. Pattern Recogn. Lett. 25(9), 1059–1065 (2004). https://doi.org/10.1016/j.patrec.2004.03.003
31. Shubham, S., Bhandari, A.K.: A generalized Masi entropy based efficient multilevel thresholding method for color image segmentation. Multimed. Tool. Appl. 78(12), 17197–17238 (2019). https://doi.org/10.1007/s11042-018-7034-x
32. Lin, J.: Divergence measures based on the Shannon entropy. IEEE Trans. Inf. Theor. 37(1), 145–151 (1991). https://doi.org/10.1109/18.61115
33. Kullback, S.: Information Theory and Statistics (1997)
34. Pare, S., et al.: An efficient method for multilevel color image thresholding using cuckoo search algorithm based on minimum cross entropy. Appl. Soft Comput. 61, 570–592 (2017). https://doi.org/10.1016/j.asoc.2017.08.039
35. Kennedy, J., Eberhart, R.: Particle swarm optimization. Neural Network. 4, 1942–1948 (1995)
36. Bhandari, A.K., Kumar, A., Singh, G.K.: Tsallis entropy based multilevel thresholding for colored satellite image segmentation using evolutionary algorithms. Expert Syst. Appl. 42(22), 8707–8730 (2015). https://doi.org/10.1016/j.eswa.2015.07.025
37. Harnrnouche, K., Diaf, M., Siarry, P.: A comparative study of various meta-heuristic techniques applied to the multilevel thresholding problem. Eng. Appl. Artif. Intell. 23(5), 676–688 (2010). https://doi.org/10.1016/j.engappai.2009.09.011

17519683, 2022, 6, Downloaded from https://ietresearch.onlinelibrary.wiley.com/doi/10.1049/sil2.12148 by Gwangju Institute of Science and Technology (GIST), Wiley Online Library on [05/09/2024]. See the Terms and Conditions (https://onlinelibrary.wiley.com/terms-and-conditions) on Wiley Online Library for rules of use; OA articles are governed by the applicable Creative Commons License

38. Passino, K.M.: Biomimicry of bacterial foraging for distributed optimization and control. IEEE Control Syst. Mag. 22(3), 52–67 (2002)
39. Das, S., et al.: Bacterial foraging optimization algorithm: theoretical foundations, analysis, and applications. Stud. Comput. Intell. 203, 23–55 (2009)
40. Singh, V.: Sunflower leaf diseases detection using image segmentation based on particle swarm optimization. Artif. Intell. Agric. 3, 62–68 (2019). https://doi.org/10.1016/j.aiia.2019.09.002
41. Yang, X.S.: Firefly algorithms for multimodal optimization. Lect. Notes Comput. Sci. 5792 LNCS, 169–178 (2009)
42. Yang, X.S., Deb, S.: Cuckoo search: recent advances and applications. Neural Comput. Appl. 24(1), 169–174 (2013). https://doi.org/10.1007/s00521-013-1367-1
43. Zhao, F., et al.: Adaptive multilevel thresholding based on multi-objective artificial bee colony optimization for noisy image segmentation. J. Intell. Fuzzy Syst. 39(1), 305–323 (2020). https://doi.org/10.3233/jifs-191083
44. Suresh, S., Lal, S.: An efficient cuckoo search algorithm based multilevel thresholding for segmentation of satellite images using different objective functions. Expert Syst. Appl. 58, 184–209 (2016). https://doi.org/10.1016/j.eswa.2016.03.032
45. Chaturvedi, R., et al.: Multi-level segmentation of fruits using modified firefly algorithm. Food Anal. Methods 1, 1–10 (2022). https://doi.org/10.1007/s12161-022-02290-7
46. Rosin, P.L.: Unimodal thresholding. Pattern Recogn. 34(11), 2083–2096 (2001). https://doi.org/10.1016/s0031-3203(00)00136-9
47. Sathya, P.D., Kayalvizhi, R.: Optimal multilevel thresholding using bacterial foraging algorithm. Expert Syst. Appl. 38(12), 15549–15564 (2011). https://doi.org/10.1016/j.eswa.2011.06.004
48. Bhandari, A.K., et al.: Cuckoo search algorithm and wind driven optimization based study of satellite image segmentation for multilevel thresholding using Kapur's entropy. Expert Syst. Appl. 41(7), 3538–3560 (2014). https://doi.org/10.1016/j.eswa.2013.10.059
49. Yin, P.Y.: Multilevel minimum cross entropy threshold selection based on particle swarm optimization. Appl. Math. Comput. 184(2), 503–513 (2007). https://doi.org/10.1016/j.amc.2006.06.057
50. Li, C.H., Lee, C.K.: Minimum cross entropy thresholding. Pattern Recogn. 26(4), 617–625 (1993). https://doi.org/10.1016/0031-3203(93)90115-d
51. Yang, X.S., Deb, S.: Cuckoo search via Lévy flights. 2009 World Congr. Nat. Biol. Inspired Comput. NABIC 2009 - Proc., pp. 210–214 (2009)
52. Yang, X., Deb, S.: Engineering optimisation by cuckoo search. Int. J. Math. Model. Numer. Optim. 1(4), 330–343 (2010). https://doi.org/10.1504/ijmmno.2010.035430

How to cite this article: Kumar, A., et al.: An improved segmentation technique for multilevel thresholding of crop image using cuckoo search algorithm based on recursive minimum cross entropy. IET Signal Process. 16(6), 630–649 (2022). https://doi.org/10.1049/sil2.12148

17519683, 2022, 6, Downloaded from https://ietresearch.onlinelibrary.wiley.com/doi/10.1049/sil2.12148 by Gwangju Institute of Science and Technology (GIST), Wiley Online Library on [05/09/2024]. See the Terms and Conditions (https://onlinelibrary.wiley.com/terms-and-conditions) on Wiley Online Library for rules of use; OA articles are governed by the applicable Creative Commons License